

STRUCTURAL BEHAVIOR OF TIMBER-STEEL-JOINTS WITH EITHER DOWEL-TYPE FASTENERS OR CONTINUOUS JOINTS

Simon Aurand¹, Jakob Boretzki², Peter Haase², Thomas Ummenhofer², Philipp Dietsch¹

ABSTRACT: For the development of a new hybrid construction method combining the materials steel and timber for linear load-carrying elements subjected to bending loads, different joining methods were investigated. The joining methods were 1) dowel-type fasteners, partly in combination with higher friction in the shear plane and 2) continuous joints, mainly by bonding with adhesives. Tests were carried out to investigate the maximum load-carrying capacity as well as the stiffness of the joints, aiming to transfer the results to the linear load-carrying elements. Where applicable, nominal shear stresses were evaluated. The tests with dowel-type fasteners were mainly carried out to create reference values to compare to the other joining methods. The results with the modified surfaces to increase friction in the shear plane were quite promising regarding the initial stiffness, however, further research of the surface modification has to be carried out. The specimens with continuous joints can be regarded analytically as fully bonded. Bonded specimens with additional bolts combine high stiffness with a residual load-carrying capacity after shear failure of the timber of 30-40% of the maximum load.

KEYWORDS: timber-steel composite beams, dowel-type fasteners, adhesive bonding, continuous joints

1 INTRODUCTION

The results presented in this paper were determined as part of an ongoing research project. Its main objective is the development of a hybrid construction method by combining the materials steel and timber for linear load-carrying elements subjected to bending loads, similar to [1, 2]. The hybrid construction method is characterized by the shear-resistant embedment of a steel profile in a compact timber cross-section, see Figure 1. The bond between the steel profile and the timber cross-section is achieved either by dowel-type fasteners, by a continuous joint or by a combination of the two methods. In this way, the specific advantages of the two materials can be utilized in an optimized manner and the weaknesses of the materials can be compensated for by the composite partner. These hybrid members enable a significant increase in the possible spans, in comparison with conventional timber structures, as they result in a considerable increase in bending stiffness. All this while maintaining compact cross-sectional dimensions. In return, the timber profiles laterally support the thin steel profile and hence prevent its buckling failure. Also, the timber encapsulates and hence protects the steel profile in case of fire.

2 MATERIAL COMBINATIONS

By analytical investigation, suitable material pairings of timber and steel were identified, that are best utilized for

different geometric configurations of the cross-section. In particular, a vertically embedded flat steel profile as well as two horizontally embedded profiles were investigated (see Figure 1). To calculate the degree of utilization of the two composite partners, a 4-point-bending test according to EN 408 [3] was chosen as static system. For simplification, full bond between the timber and steel was assumed, and that the cross-sections remain even. Characteristic values were applied in the investigation.

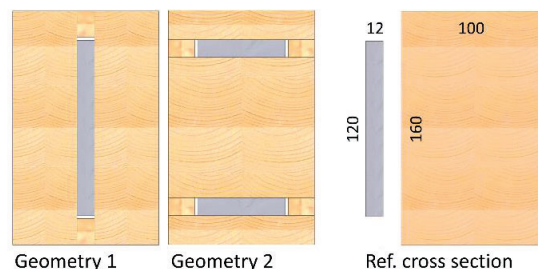


Figure 1: Exemplary timber-steel hybrid cross-sections

A variety of material combinations and cross-sections was analyzed. The investigation showed that for a low timber grade, a low steel grade is appropriate and high timber grades require high steel grades to realize equal degrees of utilization. Also, the availability of the used materials was considered. Based on the degree of utilization and the material's availability, two suitable pairings were chosen:

¹ Karlsruhe Institute of Technology (KIT), Timber Structures and Building Construction, Germany, mail: aurand@kit.edu, dietsch@kit.edu

² Karlsruhe Institute of Technology (KIT), Steel and Lightweight Structures, Germany, mail: jakob.boretzki@kit.edu, peter.haase@kit.edu, thomas.ummehofer@kit.edu

First, commonly available glulam GL24h combined with normal steel S355, and second, common softwood LVL with only parallel layers (LVL48P according to [4]) combined with high-strength steel S460. For both combinations, the degree of utilization in both composite partners was nearly identical. For the combination GL24h+S355, the timber was decisive with a utilization of 100% compared to the steel with 93%. For the combination LVL48P+S460, the steel was decisive with a utilization of 100% compared to the timber with 92% (see Table 1).

Compared to the reference cross-section of only the timber part (100 x 160 mm²), the increase in stiffness of geometry 1 with one vertical steel profile was 87% for glulam and 72% for LVL. For geometry 2 with two horizontal steel profiles, the increase in stiffness was 213% for glulam and 176% for LVL (see Table 1). The decrease of deflection at mid-span, applying the same load level as the reference cross-section, was 47% for glulam and 42% for LVL for geometry 1 and 68% for glulam and 64% for LVL for geometry 2. The results for geometry 1 were also compared to a hypothetical cross-section consisting only of the vertical steel component (12 x 120 mm²), see Table 1. Buckling failure was excluded and not further considered for the analysis.

Table 1: Exemplary results of analytical investigation

Reference cross-section	Geometry 1		Geometry 2	
	GL24h + S355	LVL48P + S460	GL24h + S355	LVL48P + S460
	Degree of utilization			
Timber:	100%	92%	100%	92%
Steel:	93%	100%	93%	100%
	Stiffness			
Timber:	+87%	+72%	+213%	+176%
Steel:	+103%	+123%	-	-
	Deflection			
Timber:	-47%	-42%	-68%	-64%
Steel:	-51%	-37%	-	-

3 JOINING METHODS AND THEIR MANUFACTURE

The studied joining methods can be categorized in two main groups:

- Dowel-type fasteners
- Continuous joints

3.1 Dowel-type fasteners

The idea behind the use of dowel-type fasteners was the wide availability of such fasteners and their ease-of-application. Especially self-tapping screws offer potential. Additionally, the possibility to increase the load-carrying capacity and especially the stiffness by modifying the steel surface was investigated.

Dowel-type fasteners commonly used in timber construction were chosen. All fasteners had a uniform outer diameter of 10 mm.

The following fasteners were investigated:

- Galvanized dowels for comparative tests
- Galvanized bolts with large washers (Ø = 50 mm)
- Partially threaded screws with a washer head (Ø = 22.5 mm) as well as a countersunk head (Ø = 17.0 mm)
- Fully threaded screws with a countersunk head (Ø = 18.5 mm)

The holes for the fasteners were drilled with a special twist drill, which allowed to drill through both materials, timber and steel without changing the drill bit. However, while drilling through the steel, the drill had to be constantly removed from the hole to allow for the clearing of the metal shavings. This resulted in a slightly greater hole diameter in one of the two side members, which was clearly noticeable when inserting the dowels, bolts, and screws. The fit of the fasteners was always tighter in the second timber side member. Also, the use of the timber-steel twist drill had the disadvantage of leaving one timber side member with a hole the size of the screws' outer diameter instead of the screws' shank diameter (for partially threaded screws) or the screws' core diameter (for fully threaded screws). This also resulted in a more loose fit of the fastener in one of the two side members. The second timber part of the specimens with screws was not pre-drilled for tests with GL24h. However, for tests with LVL48P, the second timber part was pre-drilled with 7 mm, according to their product specification [5, 6].

As mentioned before, the possibility of a surface modification in terms of higher friction in the shear plane was investigated. In [7], various surface modifications were studied, of which two surface modifications were tested in this project:

- Milled circular pattern
- Coated with quartz sand

The milling of the circular pattern into the steel surface was done by using a face mill with replaceable inserts, of which every second insert was removed. The rotational speed as well as the feed rate of the milling tool were both set quite high in order to achieve a rough circular pattern, as can be seen in Figure 2. To obtain a satisfying result, various pairings of rotational speed and feed rate were tested.

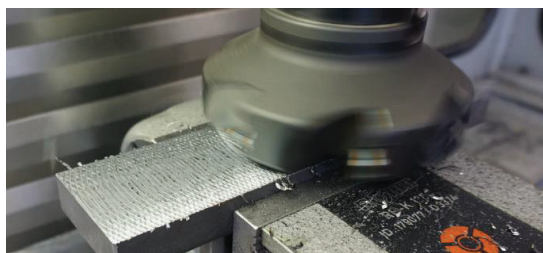


Figure 2: Milling process of circular pattern

For the coating of the steel with quartz sand a two component epoxy resin (2K EP [8]) was applied onto the steel surface. The surface was sandblasted and degreased with butanone. The adhesive layer had a thickness of ca. 0.5 mm and the quartz sand had a maximum grain size of 1 mm with about 90% of the grain size between 0.5-0.8 mm. The quartz sand was then pressed by hand into the resin and the resin cured according to the manufacturer's specification. Extracts from the manufacturing process and the final surface can be seen in Figure 3.

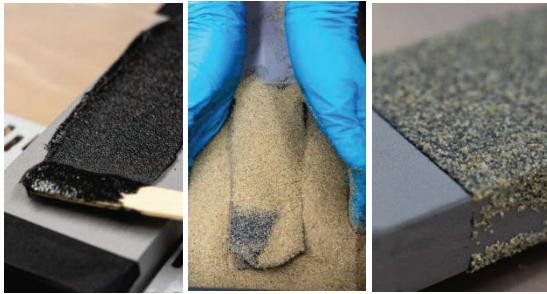


Figure 3: Manufacturing process of coated specimens

3.2 Continuous joints

The continuous joining was achieved by two different methods:

- Pressing in punched metal plate fasteners (nail plates)
- Adhesive bonding

The nail plates used consisted of 1 mm steel sheets with a nail length of 8.5 mm [9]. The nail plates were adhesively bonded to the steel surface, see Figure 4. Here, the same 2K EP was used as for the coated surface. Again, the steel and the nail plates were sandblasted and degreased before the adhesive was applied. The nail plates with the steel parts were then pressed into the timber parts. A pressing power of around 5 N/mm² was applied, partly exceeding the compressive strength perpendicular to the grain of the timber side members. This resulted in either deformed timber parts or only partially pressed-in nail plates. Therefore, the manufacturing order was changed and the nail plates were first pressed into the timber and afterwards the steel was bonded to the nail plates. Better results could also be achieved when placing the timber parts “edgewise”, i.e. pressing the nail plates in the side surface in multiple laminations/veneers.



Figure 4: Bonding of nail plates to steel parts

For the adhesive bonding of steel and timber, two different adhesives were chosen, a two component epoxy resin (2K EP [10]) and a two component polyurethane adhesive (2K PU [11]). For each combination, the respective pull-off adhesion strength was determined, see Figure 5 left. During these tests, a perpendicular force was applied to separate the bonded loading fixture from the surface. This easy and standardized test (e.g. [12]) allowed for a comparison of the adhesion properties of adhesives. Furthermore, different tools for their application were tested for both adhesives. Two requirements were pursued: an even and defined spread of the adhesive and a shape of the applied adhesive, which results in a preferably bubble-free adhesive layer. The best results were obtained with a notched spatula with 4 mm notches.

For the manufacturing of the composite test specimens, the steel parts were all sandblasted and cleaned with butanone before bonding. For the PU adhesive, a primer [13] had to be applied additionally. The timber parts were all planed directly before bonding. The bonding of the specimens was done in normal climate 20°C/65%rH.

All tests with continuous joints were performed with and without additional bolts. For the tests with additional bolts, the bolts were already used in the manufacturing process to apply the contact pressure.

A more detailed description of the selection of the adhesives and the manufacturing process of the adhesively bonded composite specimens is given in [14].

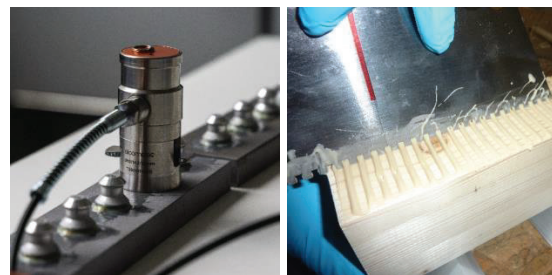


Figure 5: Pull-off adhesion tests prior to final material selection (left) and spreading of adhesive with notched spatula (right)

4 TESTS WITH STEEL-TIMBER JOINTS

4.1 TEST SETUP AND PROGRAM

Joint tests were performed to determine the joint properties. The test specimens were designed based on Johansen's yield theory [15] with two shear planes for each fastener (see Figure 6). The timber parts were dimensioned in such a way, e.g. with an end distance $a_{3,t} = 7d = 70$ mm, that failure of the fasteners occurred with two plastic hinges per shear plane. The density of both timber side members was equal. An overview of the performed tests is given in Table 2. In total, 100 tests were performed of which an excerpt is presented in the following.

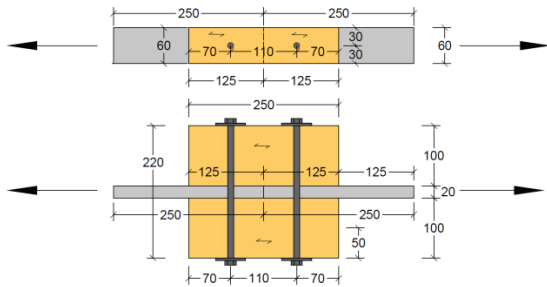


Figure 6: Test specimens

The joint tests were performed according to EN 26891 [16] with an unloading loop. Each test was stopped after failure of the specimen or after reaching a displacement of 15 mm in one of the shear planes. For all specimens and all shear planes, the relative displacement between the timber and the adjacent steel part was measured continuously. For this, a digital image correlation (DIC) system [17] was used, see Figure 7. The DIC system repeatedly took pictures of the test specimen with applied markers and the software calculated the displacement of the markers in each frame.

Table 2: Number of tests for different joining methods and two different timber grades

No.	Joint	GL24h	LVL48P
1	Dowels	3	3
2	Bolts	4	-
3	Bolts + milled surface	3	-
4	Bolts + coated surface	5	-
5	Screws A ¹⁾ (countersunk head)	3	-
6	Screws B ²⁾ (washer head)	3	3
7	Screws C ³⁾ (countersunk head)	3	3
8a	Nail plates	3	3
8b	Nail plates + bolts	2	-
9a	2K EP	5	5
9b	2K EP + bolts	5	5
10a	2K PU	5	5
10b	2K PU + bolts	5	5

¹⁾ partially threaded screws with countersunk head

²⁾ partially threaded screws with washer head

³⁾ fully threaded screws with countersunk head

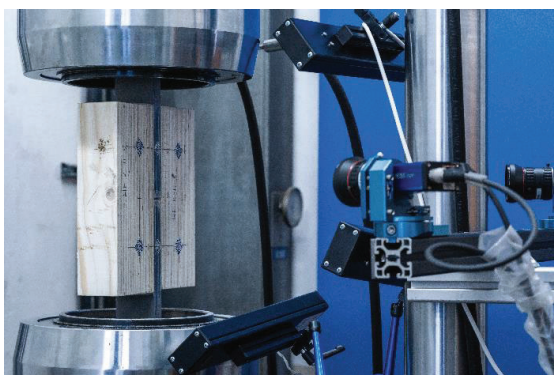


Figure 7: Test setup with digital image correlation (DIC) system

4.2 TEST RESULTS AND DISCUSSION

4.2.1 General

For each specimen, the maximum load F_{\max} per shear plane was evaluated. The stiffness k_s was evaluated separately for all four shear planes in the range between 10-40% of F_{\max} , unless otherwise stated. In order to take into account the influence of the manufacturing process as well as the surface treatment, the stiffness k_i was additionally evaluated in the range of 0-40% of F_{\max} . On the one hand, the influence of the larger borehole diameter is shown for the test specimens with screws, and on the other hand, the influence of the surface treatment is taken into account for the test specimens with the roughened surfaces. The results for all tests with dowel-type fasteners are given in Table 3 and the exemplary load-displacement curves in Figure 10. For all tests with continuous joints, the results are given in Table 4 and exemplary load-displacement curves in Figure 14. The force F_{\max} is the mean value of all three to five tests of one series per fastener and shear plane. The stiffness k_i and k_s is the mean value of all four shear planes and all tests of one series. For the specimens with continuous joints, a nominal shear stress f_v was evaluated. The shear stress was calculated with the mean value of F_{\max} of all tests of one series and the generalized area of the shear plane, i.e. 60 mm x 125 mm less the hole diameter, for tests with fasteners. To better compare the different joining methods, the nominal shear stress was also evaluated for the specimens with dowel-type fasteners, although no shear failure occurred. The timber parts were stored at normal climate 20°C/65%rH and mean moisture contents of $u = 10\%$ for glulam and $u = 8.7\%$ for LVL were evaluated. The density of the glulam specimens varied between 388 and 488 kg/m³ and for LVL between 483 and 643 kg/m³ (see Table 3 and Table 4).

4.2.2 Tests with dowel-type fasteners

The reference tests with GL24h+S355 and dowels reached a mean load of 10.6±0.47 kN and a mean stiffness k_i of 3.97±1.16 kN/mm and with LVL48P+S460 a mean load of 14.9±0.33 kN and a mean stiffness k_i of 8.32±1.21 kN/mm. The stiffness k_s was evaluated between 20-50% of F_{\max} and k_i between 0-50%. The specimens failed by splitting of one of the timber side members, before reaching a relative displacement of 15 mm in any of the four shear planes. The designed failure with two plastic hinges per shear plane was reached. However, for some dowels, the plastic hinges were barely visible. This leads to the assumption that the end distance $a_{3,t} = 7d = 70$ mm was not large enough.

The tests with bolts and large washers reached a mean load of 14.6±1.59 kN and a mean stiffness k_i of 5.85±1.65 kN/mm. The stiffness k_s was evaluated between 30-60% of F_{\max} and k_i between 0-60%. Here, the two plastic hinges were clearly visible. Splitting of the timber occurred as well, however, did not result in a decrease of the load. Whereas the tests with dowels showed some initial slip, the tests with bolts and washer showed no slip at all because of the pre-stressing from tightening the nut. The slightly higher stiffness k_s of the dowel joints (see Table 3) might be due to the fact, that

the actual dowels' diameter was measured with $d = 10.0$ mm, while the bolts' actual diameter was only 9.4 mm, thus resulting in a tighter fit of the dowel joint.

The tests with bolts and modified surfaces both reached slightly higher results with $F_{max} = 17.1 \pm 0.60$ kN for the milled surface and 18.3 ± 2.58 kN for the coated surface. The stiffness amounted to $k_i = 4.82 \pm 0.80$ and 5.80 ± 1.06 kN/mm, respectively. For the tests with the milled surface, the stiffness k_s was evaluated between 40-60% of F_{max} and k_i between 0-60%. For the tests with the coated surface, the stiffness k_s was evaluated between 30-50% of F_{max} and k_i between 0-50%. The load-displacement curves showed a significantly higher initial stiffness, due to the increased friction between steel and timber. The tests with the milled surface remained in stick state up to almost one third of the total load, which is quite astonishing as there is almost no visible damage to the timber surface, as can be seen on the left in Figure 8. This was not the case for the tests with the coated surface, where large deformations were needed to properly press the quartz sand into the timber surface, which then led to high abrasion of timber fibers, as can be seen on the right in Figure 8. However, the tests showed that a surface modification in combination with laterally loaded fasteners is not as promising as in combination with mainly axially loaded fasteners, see [7].



Figure 8: Milled surface with almost no abrasion and no damage to the timber surface (left) and coated surface with high abrasion of timber fibers (right)

The tests with partially threaded screws reached the lowest loads with $F_{max} = 9.89 \pm 0.39$ kN for the screws with a countersunk head and 11.2 ± 0.98 kN for the screws with a washer head. The stiffness was also quite low with $k_i = 1.27 \pm 0.10$ (countersunk head) and 1.29 ± 0.15 kN/mm (washer head). The stiffness k_s was evaluated between 20-50% of F_{max} and k_i between 0-50%. The low results can be explained with the manufacturing process of the specimens, where a 10 mm hole was drilled through one timber side member and through the steel. So for the smooth shank to be in contact with the timber, approximately 1.5 mm displacement had to be reached first. This also resulted in the formation of only one plastic hinge per shear plane on the side of the shank, as can be seen in Figure 9.

The fully threaded screws performed better with a mean load of 16.5 ± 0.41 kN for GL24h and 18.9 ± 1.60 kN for LVL48P and a mean stiffness k_i of 2.90 ± 0.39 kN/mm and 4.35 ± 0.84 kN/mm, respectively. The stiffness k_s was evaluated between 10-35% of F_{max} and k_i between 0-35%.



Figure 9: Partially threaded screws after tests with countersunk head (left) and washer head (right)

The coefficient of variation (COV) of the resulting maximum loads is within the expected range with 2% to 14% for GL24h and 2% to 8% for LVL48P. The COV of the evaluated stiffness values is significantly higher with 7% to 35% for GL24h and 12% to 26% for LVL48P, again as expected. In general, the tests showed that screws are not able to provide the desired composite properties in this project. The maximum loads are mainly reached at large displacements of 15 mm, see also Figure 10. The stiffness is correspondingly low and feature a large scatter, see also Figure 11.

Table 3: Maximum load F_{max} , stiffness k_i and k_s , and shear stress f_v per fastener and shear plane for joints with dowel-type fasteners (incl. standard deviation and COV in %)

No.	F_{max} kN	k_i kN/mm	k_s kN/mm	f_v N/mm ²	ρ kg/m ³
GL24h					
1	10.6	3.97	6.36	1.43	446
	0.47	1.16	1.30	0.06	7.14
	4%	29%	20%	4%	2%
2	14.6	5.85	4.37	1.97	466
	1.59	1.65	1.05	0.21	11.4
	11%	28%	24%	11%	2%
3	17.1	4.82	3.97	2.31	452
	0.60	0.80	1.15	0.08	4.21
	3%	17%	29%	3%	1%
4	18.3	5.80	5.65	2.46	431
	2.58	1.06	1.80	0.35	19.1
	14%	18%	32%	14%	4%
5	9.89	1.27	1.68	1.33	440
	0.39	0.10	0.59	0.05	1.00
	4%	7%	35%	4%	0%
6	11.2	1.29	1.76	1.50	443
	0.98	0.16	0.12	0.13	1.50
	9%	12%	7%	9%	0%
7	16.5	2.90	2.60	2.22	478
	0.41	0.39	0.33	0.06	-
	2%	13%	13%	2%	-
LVL48P					
1	14.9	8.32	9.56	2.01	641
	0.33	1.21	1.15	0.04	1.26
	2%	15%	12%	2%	0%
6	13.7	1.72	1.99	1.85	625
	0.92	0.29	0.49	0.12	20.3
	7%	17%	25%	7%	3%
7	18.9	4.35	4.14	2.54	613
	1.60	0.84	1.06	0.22	7.03
	8%	19%	26%	8%	1%

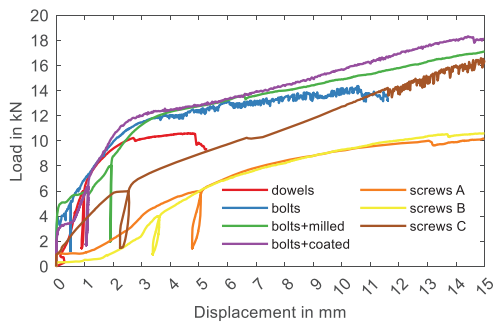


Figure 10: Load-displacement curves for all tests with dowel-type fasteners and material combination GL24h + S355J2

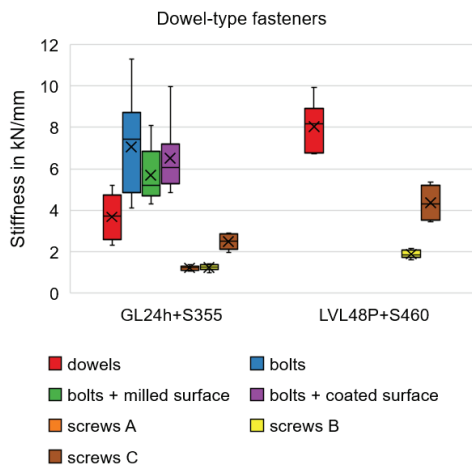


Figure 11: Stiffness for all tests with dowel-type fasteners and both material combinations

4.2.3 Tests with continuous joints

The tests with the nail plates resulted in a higher maximum load $F_{\max} = 21.3 \pm 0.47$ kN and a significantly higher stiffness $k_i = 116 \pm 46.2$ kN/mm. The specimens failed brittle by shear failure in the timber, in the plane of the nail tips, see Figure 12. A nominal shear stress of $f_v = 2.84 \pm 0.06$ N/mm² was evaluated. For the tests with additional bolts, the maximum load increased to $F_{\max} = 26.2 \pm 3.78$ kN, the stiffness however decreased to $k_i = 84.1 \pm 21.7$ kN/mm. This might be due to the fact, that the size of the nail plates decreased by the bolt's cross-section, thus decreasing the joined area. Again, the specimens failed by shear failure of the timber side members. Here, the evaluated shear stress was 3.53 ± 0.51 N/mm². The lower shear stress for the tests without bolts might be due to the fact that these were the first specimens, where the nail plates were not properly pressed in, thus reducing the area to transfer loads. After initial failure, the load-carrying capacity dropped to about half the maximum load. Splitting of the side members occurred, but was regarded as secondary failure. Exemplary tests showed that the load-carrying capacity could be further increased if the timber parts were oriented "edgewise" thus pressing the nail plates in multiple laminations/veneers.



Figure 12: Failed specimen of test with nail plates, glulam and additional bolts (left) and test with nail plates and LVL (right)

The tests with bonded specimens reached the highest loads with $F_{\max} = 24.8 \pm 4.19$ kN for the 2K EP and 29.3 ± 4.38 kN for the 2K PU. Stiffness values of $k_i = 655 \pm 166$ kN/mm and 464 ± 63.3 kN were evaluated. The displacements at the time of failure were very small with only 0.2 mm. Shear failure occurred in the timber mainly very close to the contact surface with the steel (see Figure 13). Shear stresses of 3.31 ± 0.56 N/mm² and 3.90 ± 0.58 N/mm² were evaluated for the two adhesives. Again, for the tests with additional bolts, the load-carrying capacity dropped to about 30 kN after the shear failure occurred, which approximately was the maximum load of the tests on solely bolted joints. The load level then only slightly increased with increasing displacement. At a displacement of 15 mm, the tests were terminated.

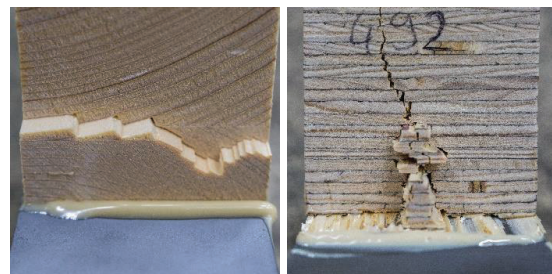


Figure 13: Failed specimen of test with 2K EP and glulam (left) and test with 2K PU, LVL and bolt (right). Splitting was secondary failure and occurred after sudden shear failure

In general, no differences of the used adhesives could be observed in the test results. In Figure 14, load-displacement curves for the tests with continuous joints are given. Because of the very small displacements at the time of failure of the adhesively bonded specimens paired with the ductile behavior and large deformations of the specimens with additional bolts, the scale of the x-axis is split into two sections with different intervals.

The COV of the resulting maximum loads is within the expected range with 2% to 17% for GL24h and 8% to 11% for LVL48P. The COV of the evaluated stiffness values is significantly higher for GL24h with 6% to 40%, as expected and rather low for LVL48P with 8% to 19%, see also Figure 15. Because of the very small displacements at the time of failure, the measurement uncertainty has to be considered and will be evaluated in future steps.

Table 4: Maximum load F_{max} , stiffness k_i and k_s , and shear stress f_v per fastener and shear plane for continuous joints (incl. standard deviation and COV in %)

No.	F_{max} kN	k_i kN/mm	k_s kN/mm	f_v N/mm ²	ρ kg/m ³
GL24h					
8a	21.3 0.47 2%	116 46.2 40%	106 35.2 33%	2.84 0.06 2%	448 8.37 2%
8b	26.2 3.78 14%	84.1 21.7 26%	72.3 15.0 21%	3.53 0.51 14%	466 31.1 7%
9a	24.8 4.19 17%	655 166 25%	610 176 29%	3.31 0.56 17%	423 1.14 0%
9b	33.0 3.74 11%	464 63.3 14%	435 35.4 8%	4.44 0.50 11%	425 21.3 5%
10a	29.3 4.38 15%	584 47.2 8%	589 77.8 13%	3.90 0.58 15%	427 16.3 4%
10b	32.7 2.51 8%	552 33.2 6%	556 46.2 8%	4.41 0.34 8%	425 6.25 1%
LVL48P					
8b	24.2 2.61 11%	311 59.4 19%	284 40.9 14%	3.26 0.35 11%	630 1.28 0%
9a	27.6 2.95 11%	514 42.8 8%	492 50.1 10%	3.72 0.40 11%	492 3.6 1%
9b	32.0 2.87 9%	506 51.8 10%	480 46.3 10%	4.26 0.38 9%	492 3.87 1%
10a	28.8 2.45 8%	489 48.6 10%	464 49.9 11%	3.89 0.33 8%	491 5.13 1%
10b	30.1 2.73 9%	457 51.7 11%	432 54.8 13%	4.02 0.36 9%	490 4.57 1%

An in-depth presentation of the test results and subsequent discussion is given in [14].

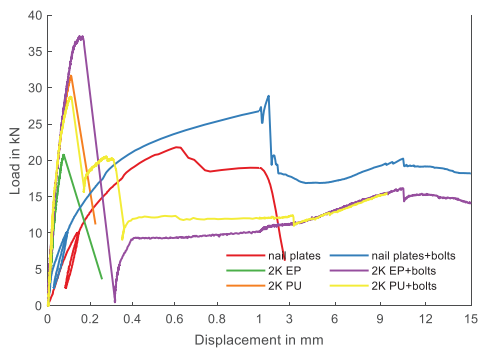


Figure 14: Load-displacement curves for all tests with continuous joints and material combination GL24h+S355J2

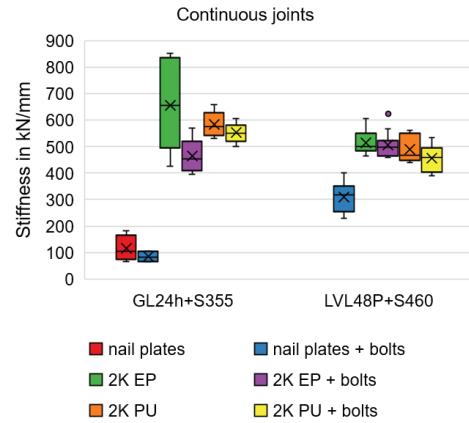


Figure 15: Stiffness for all tests with continuous joints and both material combinations

5 SUMMARY AND OUTLOOK

The test results give a comprehensive overview of the different joining methods studied in this research project on hybrid timber-steel beams. All tests were carried out with the same sized specimens. The outer diameter for all dowel-type fasteners was the same, as well as the bonded area for the tests with continuous joints. The tests showed that dowel-type fasteners are not suitable for the desired purpose. Also, both surface modifications did not have the desired effect and only slightly increased the results. For the joining methods with continuous joints, fully bonded hybrid beams under bending load can be assumed. The tests also revealed valuable information about the use of bolts with bonded joints and the ductile behavior after initial shear failure of the timber.

In a further step, the behavior of the joining methods under varying environmental conditions is to be investigated. In future tests, the specimens are subjected to changing climatic conditions while simultaneously being loaded with a percentage of the load established in the here presented tests. Here, the climatic conditions of service class 1 (dry conditions, indoor environment) as well as service class 2 (more humid conditions, protected outdoor environment) are of interest.

For adhesives, the surrounding temperature is also of great importance. Each adhesive has its own specific glass transition temperature, which characterizes the range of temperature above which the glassy, brittle adhesive becomes rubbery and ductile. Once the glass transition temperature is reached, the adhesive's mechanical properties are reduced significantly. Also, the material properties of timber decrease with increasing temperature. Therefore, tests with high temperatures and adhesively bonded specimens will be performed in future tests.

Following the small scale tests with the different joining methods, full scale tests of timber-steel-composite beams are planned. In this realm, the two geometries presented in chapter 2 will be tested. The cross-sections and the dimensions of the beams will be analogous to the analytical investigation. The four-point bending tests will be performed according to EN 408.

REFERENCES

- [1] Winter W., Riola-Parada F.: Timber-Steel Hybrid Beams for Multi-Storey Buildings: Final Report. In: *World Conference on Timber Engineering WCTE 2016*. Vienna, Austria; 2016.
- [2] Tsai M.-T., Le T.: Determination of Initial Stiffness of Timber-Steel Composite (TSC) Beams Based on Experiment and Simulation Modeling. *Sustainability* 10(4):1220; 2018.
- [3] EN 408:2012-10: Timber structures - Structural timber and glued laminated timber - Determination of some physical and mechanical properties; German version; 2012.
- [4] Finnish Woodworking Industries Federation: LVL Handbook Europe. Helsinki; 2020.
- [5] ETA-19/0553: HECO-TOPIX-plus (or HTP or HT-plus), HECOTOPIX-plus-T (or HTP-T or HT-plus-T) and HECOTOPIX-plus-CC (or HTP-CC or HT-plus-CC) screws; ETA-Danmark A/S; 2021.
- [6] ETA-11/0190: Würth self-tapping screws; Deutsches Institut für Bautechnik (DIBt); 2018.
- [7] Aurand, S., Blass, H.-J.: Connections with inclined screws and increased shear plane friction. Proceedings of: *International Network on Timber Engineering Research INTER 54*. Paper 54-7-5. Online; 2021.
- [8] Product data sheet: Sikadur®-370 (Provisional); Sika Services AG, Zurich, Switzerland; 2016.
- [9] Allgemeine bauaufsichtliche Zulassung Z-9.1-761: Nagelplatte M 20 H als Holzverbindungsmittel; Deutsches Institut für Bautechnik (DIBt); 2015.
- [10] Technical data sheet: Jowat® Epoxidharz 692.30; Jowat SE, Detmold, Germany; 2019.
- [11] Technical data sheet: LOCTITE CR821 PURBOND; Henkel AG & Co. KGaA, Düsseldorf, Germany; 2022.
- [12] EN ISO 4624:2016-08: Paints and varnishes - Pull-off test for adhesion (ISO 4624:2016); German version; 2016.
- [13] Technical data sheet: BONDERITE M-NT 1455-W; Henkel AG & Co. KGaA, Düsseldorf, Germany; 2017.
- [14] Haase, P., Boretzki, J., Albiez, M., Aurand, S., Sandhaas, C., Ummenhofer, T., Dietsch, P.: Influence of the joining technique on the structural behaviour of hybrid timber-steel components. Under review for *Wood Material Science & Engineering*; 2023.
- [15] Johansen, K.W.: Theory of timber connections. *International Association for Bridge and Structural Engineering*. 9, 249-262; 1949.
- [16] EN 26891:1991-07: Timber structures; joints made with mechanical fasteners; general principles for the determination of strength and deformation characteristics (ISO 6891:1983); German version; 1991.
- [17] Q400 DIC Digital Image Correlation – non contact 3D deformation sensor; LIMESS Messtechnik und Software GmbH, Krefeld, Germany; 2023.